

Supporting Information for

A Nonsolvolytic Fluorine/LiNO₃-containing Electrolyte for Stabilizing Dynamic Interfaces in Li||LiMn₂O₄ Batteries

Tian Tang¹, J.X. Kent Zheng², Nyalaliska W. Utomo³, Lynden A. Archer^{3*}

1. Department of Materials Science and Engineering, Cornell University, Ithaca, NY, 14853, USA.

2. Department of Physics, Massachusetts Institute of Technology, Cambridge, MA, 02139, USA.

3. Robert Frederick Smith School of Chemical and Biomolecular Engineering, Cornell University, Ithaca, NY, 14853, USA.

** Corresponding author: laa25@cornell.edu*

Materials and methods

Materials

LiPF₆ and lithium bis(trifluoromethanesulfonyl)imide (LiTFSI), LiClO₄, LiMn₂O₄ were purchased from Sigma Aldrich. LiBF₄, LiNO₃, 750 μm lithium foil were purchased from Alfa Aesar. Plain carbon cloth 1071 was purchased from Fuel Cell Store. Ketjen Black carbon was purchased from AkzoNobel. The cathodes are fabricated according to the protocol we reported in an earlier work (LiMn₂O₄ content = 80 wt%).¹ Areal mass loading of the cathodes is ~3 mg/cm².

Characterization of materials

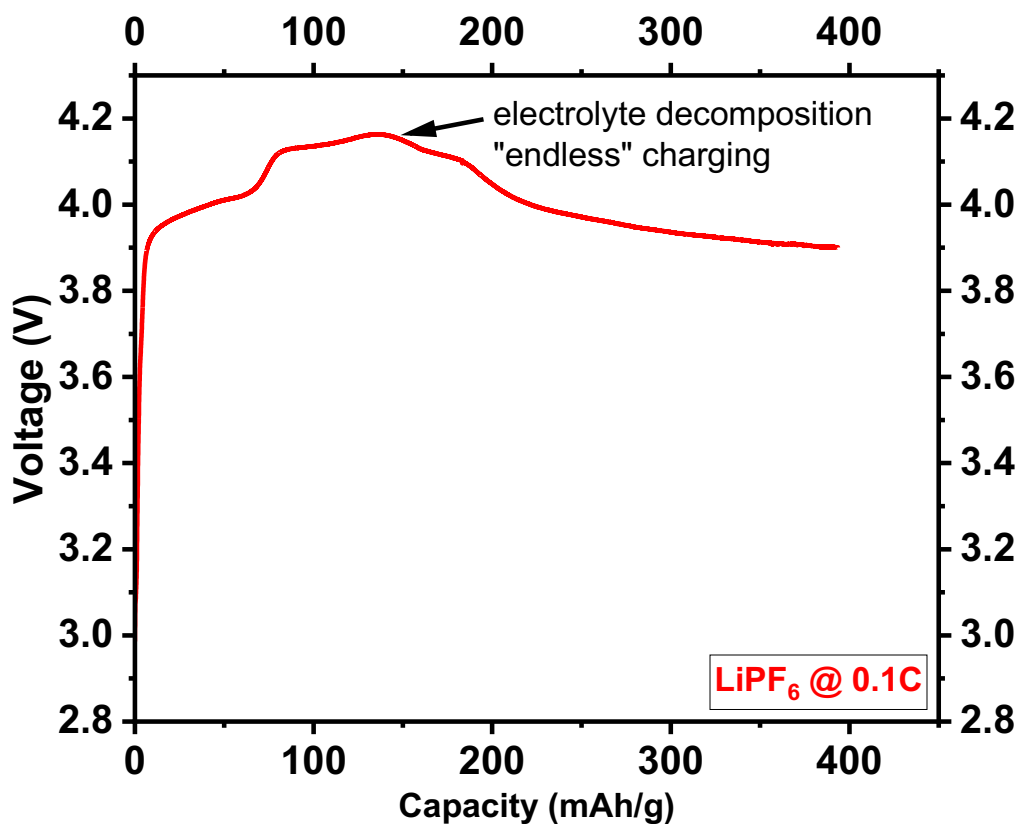
Scanning electron microscopy (SEM) was carried out on Zeiss Gemini 500 Scanning Electron Microscope equipped with Bruker energy dispersive spectroscopy (EDS) detector. Scanning transmission electron microscopy analyses were performed on a Titan Themis Z G3 Cs-Corrected S/TEM system at MIT.nano Characterization Facility. X-ray diffraction patterns were collected on a Rigaku SmartLab system with a Cu Kα incident irradiation. Synchrotron scattering is performed at 5-BM-C at Advanced Photon Source, Argonne. The electrolyte conductivity was measured through dielectric relaxation spectroscopy (DRS). Differential Scanning Calorimetry (DSC) was adopted to evaluate thermal transitions on TA Instruments Q2000. The thermal transitions were measured under nitrogen flow at a fixed ramp rate of 10 °C/min.

Electrochemical measurements

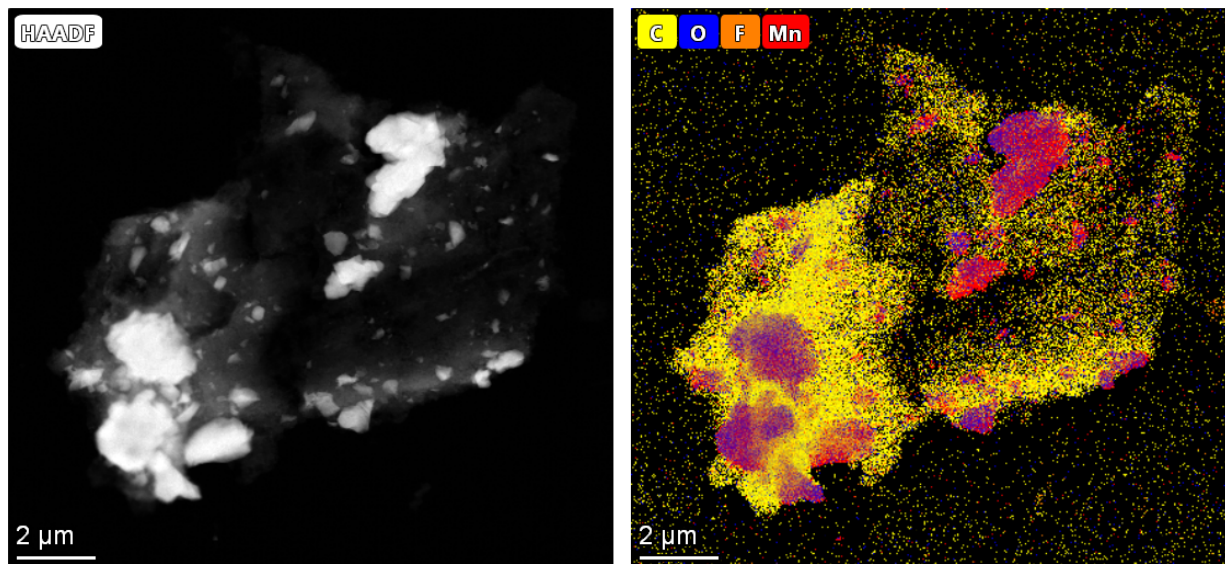
Galvanostatic charge/discharge performance of coin cells were tested on Neware battery test systems at room temperature at 1C during 3.0-4.3 V (vs. Li/Li⁺) unless specified. Electrochemical studies were

performed using CR2032 coin cells. The area of electrodes in this study is 0.71 cm^2 . Electrodes are separated by Celgard 3501. $\sim 100 \text{ }\mu\text{L}$ electrolyte is added into each cell using pipette. Electrolytes were prepared by mixing 1 M of a Li salt, 0.5 M LiNO_3 and ethylene carbonate. The coin cell (CR2032) was assembled in an argon-filled glove box. In a lithium plating/stripping Coulombic efficiency measurement (using a $\text{Li}||\text{Cu}$ cell), 1 mAh/cm^2 lithium metal is plated on the substrate from the electrolyte of interest at

$$1 \text{ mA/cm}^2. \text{ Coulombic efficiency} = \frac{\text{stripping capacity}}{\text{plating capacity}} \times 100\%.$$

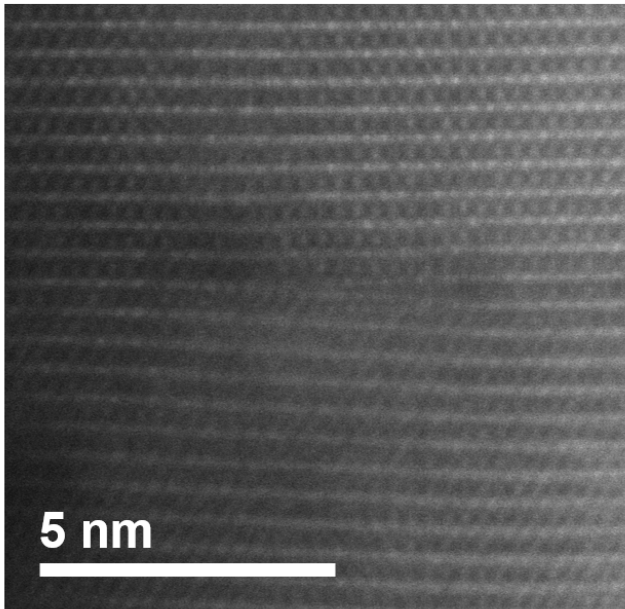


Supplementary Figure 1. Voltage profile of a Li||LiMn₂O₄ cell with LiPF₆-based electrolyte charged at 0.1C. This small current density means that any electrolyte decomposition can contribute a faradic current on this order of magnitude. In this case, the faradic current for any electrolyte decomposition can contribute a larger amount of the total current density compared with using a large current density. Considering the absence of corrosion features upon visual examination and the fact that LiMn₂O₄ is known to be catalytic, we tend to attribute that endless charging plateau to electrolyte decomposition.

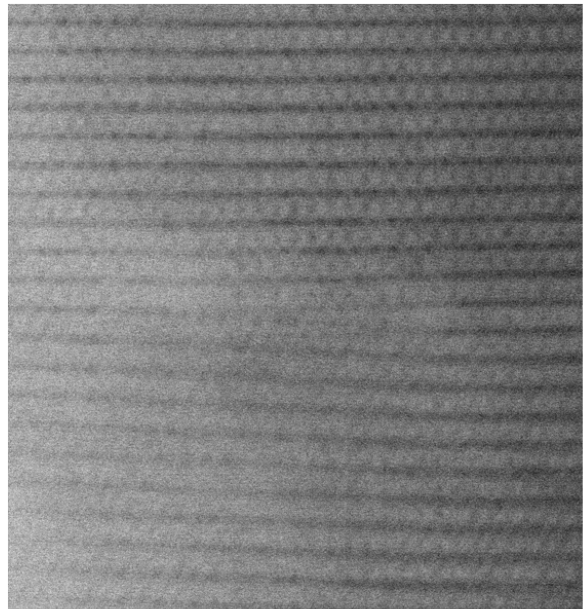


Supplementary Figure 2. STEM-EDS characterization of the electrode material. The HAADF image shown on the left and the EDS mapping shown on the right demonstrate a uniform dispersion of LiMn_2O_4 particles within a percolated carbon network (ketjen black).

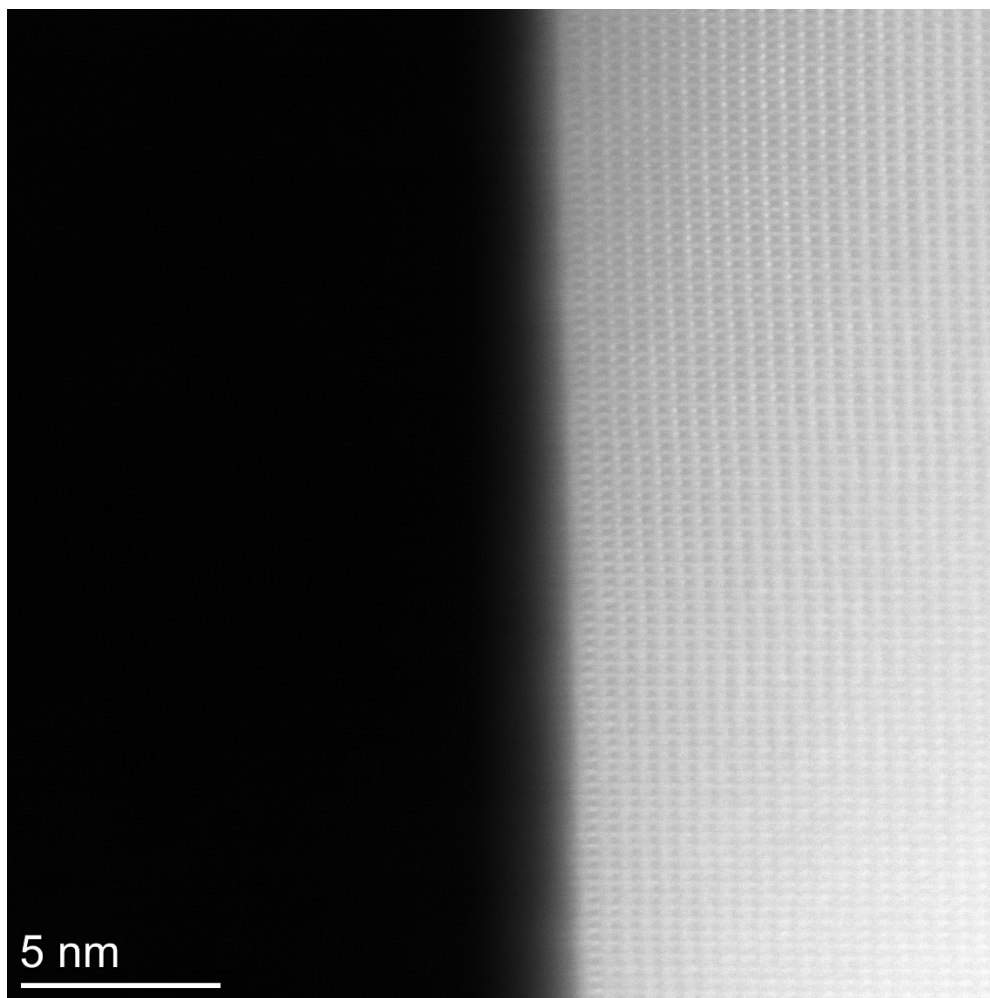
HAADF



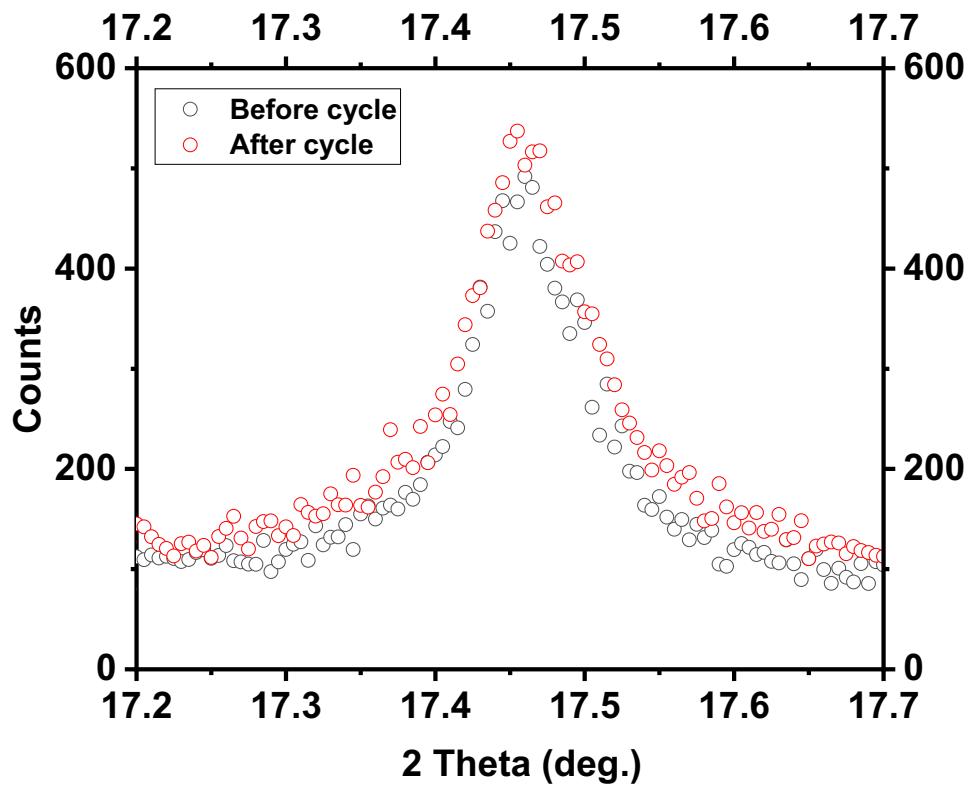
BF



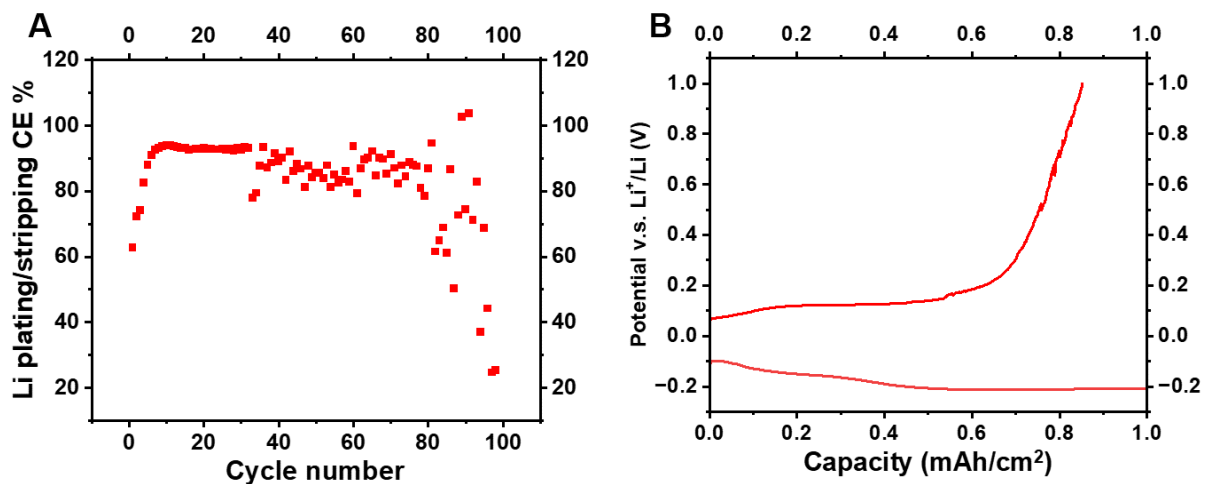
Supplementary Figure 3. High magnification STEM characterization of the defects found in LiMn_2O_4 cycled in LiPF_6 electrolyte. Clearly, the images show an edge dislocation with an extra (111) half plane.



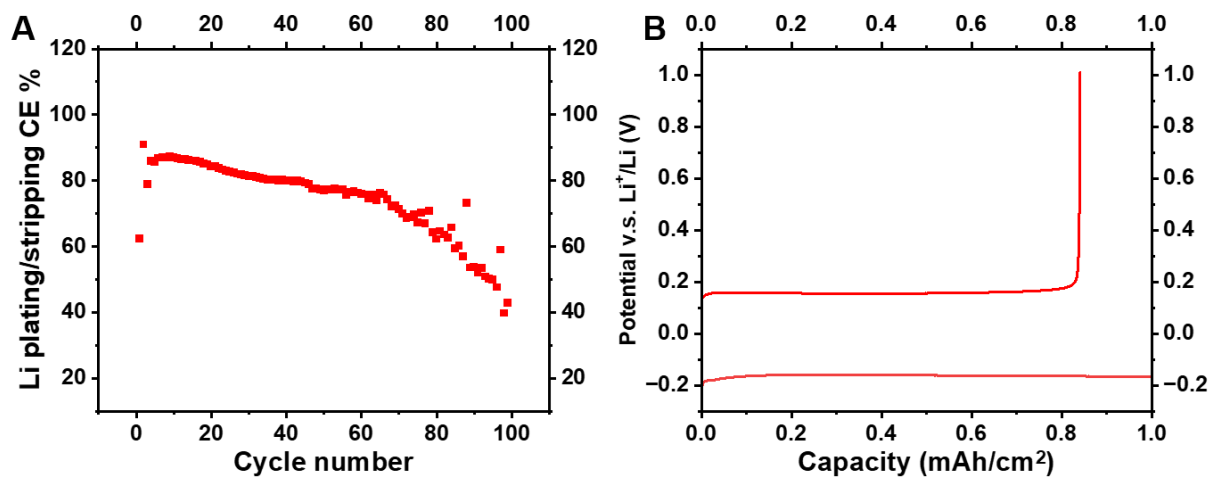
Supplementary Figure 4. HAADF-STEM image of LiMn₂O₄ cycled in LiTFSI electrolyte. The particle shows a clean, well-defined (111) terminated facet.



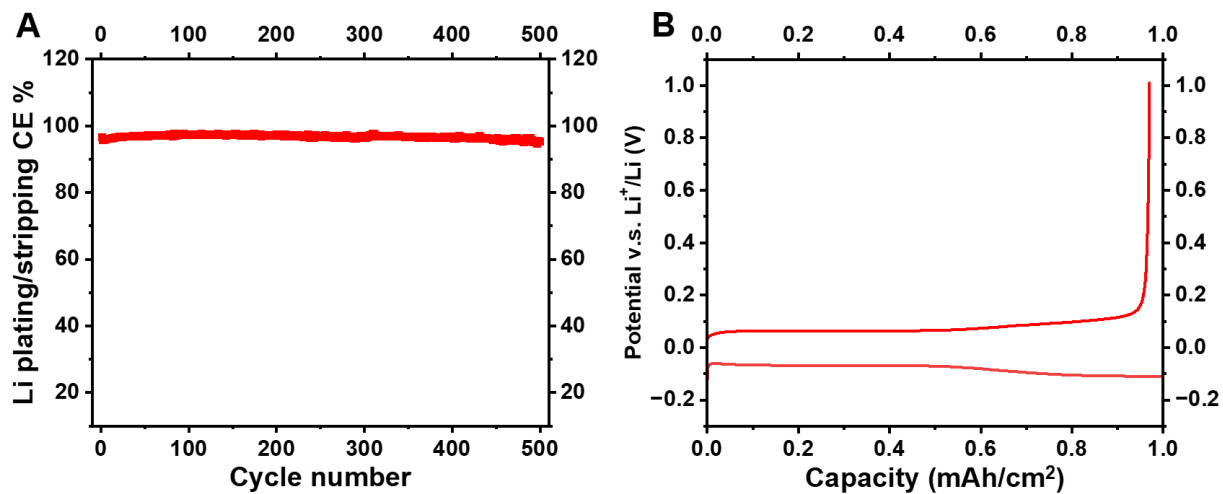
Supplementary Figure 5. Synchrotron diffraction patterns LiMn_2O_4 electrodes. Patterns of the LiMn_2O_4 electrodes before cycling (black) and after 200 cycles (red), respectively.



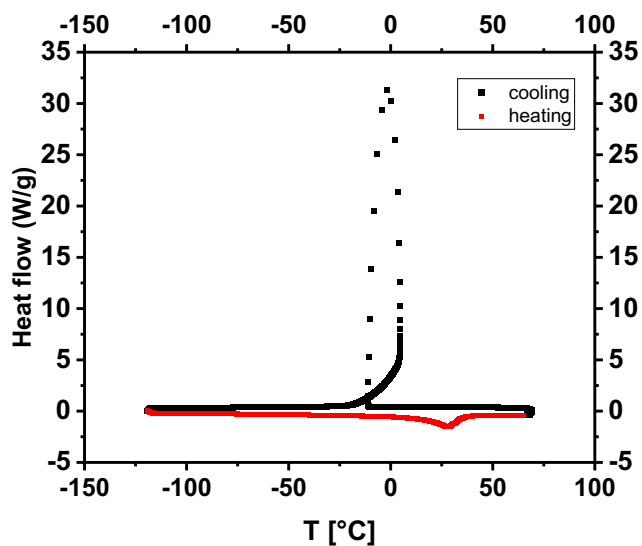
Supplementary Figure 6. Evaluation of Li plating/stripping in the LiClO_4 -based EC electrolyte. (A) CE values over cycling. (B) Representative potential profile a plating/stripping cycle.



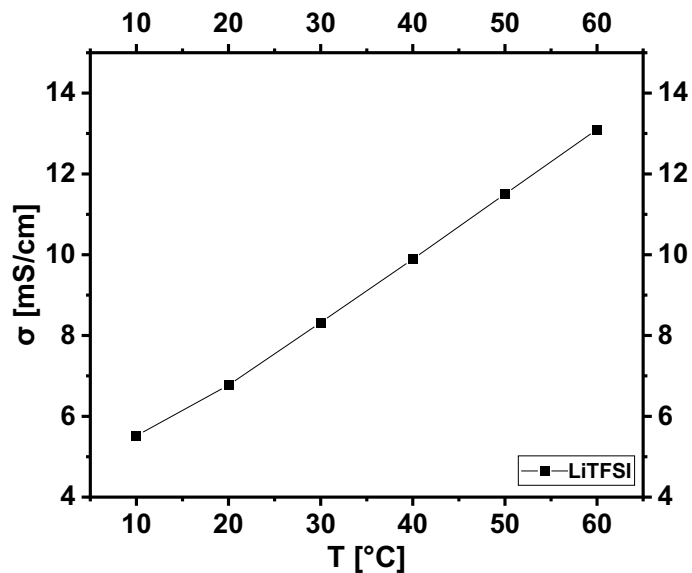
Supplementary Figure 7. Evaluation of Li plating/stripping in the LiPF₆-based EC electrolyte. (A) CE values over cycling. (B) Representative potential profile a plating/stripping cycle.



Supplementary Figure 8. Evaluation of Li plating/stripping in the LiTFSI-based EC electrolyte. (A) CE values over cycling. (B) Representative potential profile a plating/stripping cycle.



Supplementary Figure 9. DSC curve of LiTFSI-based EC electrolyte. The thermal history is removed by doing a ramp up to 70 °C, then cooling to -120 °C and having a subsequent heating to 70 °C. The data shown is the second cooling and third heating. The crystallization loop is observed and this artifact is due to the large exotherm of EC crystallization. The competition between self-heating and crystallization process leads to the loop. The melting temperature T_m obtained from the curve is 27.7 °C.



Supplementary Figure 10. Temperature-dependent conductivities of LiTFSI-based EC electrolyte probed through DRS. The ionic conductivities of the LiTFSI-based electrolyte show no clear inflection of the conductivities curve to at least 60 °C. This proves there is no decomposition of LiTFSI in this controlled atmosphere.

References

- 1 Zheng, J. *et al.* Nonplanar Electrode Architectures for Ultrahigh Areal Capacity Batteries. *ACS Energy Letters* **4**, 271-275 (2018).